Progress toward science results with the ACES spectrograph

Robert O. Reynolds[a], Michael Lloyd-Hart[a], Michael P. Lesser[a], Matthew A. Kenworthy[b], Jian Ge[c]

[a]Steward Observatory, University of Arizona, Tucson, AZ, 85721
[b]Department Of Physics, University Of Cincinnati, Cincinnati, OH, 45221
[c]Department Of Astronomy & Astrophysics, Penn State University, University Park, PA, 16802

ABSTRACT

The use of spectrographs with telescopes having high order adaptive optics (AO) systems offers the possibility of achieving near diffraction-limited spectral resolution on ground-based telescopes, as well as important advantages for instrument design. The small stellar image diameters obtained with adaptively corrected systems allow high resolution without a large loss of light at the spectrograph entrance slit, as well as greater spectral coverage per exposure. The adaptively corrected echelle spectrograph (ACES), designed at Steward Observatory for a spectral resolution R ≈ 200,000, couples the telescope pupil to the instrument with a 10 μm diameter near single-mode optical fiber. Initial observations at the 2.5m telescope on Mt. Wilson validated the concept of achieving high spectral resolution with an adaptively corrected telescope and fiber coupled spectrograph. However the transmission of multiple modes in the fiber lead to a wavelength-dependent variation in illumination that made flat fielding impossible. In this paper we describe instrument design improvements, the installation and testing of a new CCD detector, and testing aimed at understanding and eliminating the fiber-related transmission problems to permit science quality imaging.

Keywords:
Spectrograph, adaptive optics, echelle, optical fiber, single mode fiber, modal noise, CCD

1. INTRODUCTION

The ACES echelle spectrograph was developed to test the concept of optimizing a spectrograph for use strictly with adaptively corrected images. The first prototype instrument utilized an R2 echelle grating in near Littrow mode and a slit feed. Testing of the instrument at the 1.5m AO equipped telescope at Starfire Optical Range achieved spectral resolutions of R ≈ 660,000 using a HeNe laser source, and 250,000 using a stellar source and 100μm slit width.[1,2] Coupling the telescope pupil to the next generation instrument with an optical fiber permitted greater freedom in placement of the instrument, as well as azimuthal scrambling of the input illumination function.[3] The slit was replaced with a near single-mode fiber feed, and initial observations made at the 2.5m AO telescope on Mt. Wilson showed R=190,000, total wavelength coverage of ~650nm, and fiber transmission efficiency of ~70%. However, problems with fiber alignment stability limited system throughput, and the spectrograph etendu (the product of the area of an optical element and the solid angle accepted by the element) did not match that of the input fiber, also limiting throughput. The present configuration, described in Section 3, was conceived to correct those problems while providing a cost effective design. Initial observations made at Mt. Wilson in 2000 showed R=190,000 with two and a half pixel sampling, but also identified a fiber transmission problem which resulted in irradiance modulation along the echellogram orders. Similar effects have been described in instruments fed by multimode fibers, and techniques have been demonstrated for eliminating the modulation in those cases.[5] However, preliminary testing of similar techniques has shown that that approach may not be applicable to the near single-mode fiber feed used on ACES.[6] In an unrelated development, damage to the Loral CCD used in 2000 necessitated procurement and integration of an alternate detector, details of which are provided in Section 4 of this paper. Successful commissioning of the new detector and solution of the fiber transmission problem, along with improved calibration, will permit the instrument to reach its full potential at the Mt. Wilson telescope. We then anticipate observing runs at other AO equipped telescopes such as the 3.5m at Starfire Optical Range (SOR) and the 3.67m AEOS on Maui before permanent installation of the instrument at the 6.5m MMT in Arizona.

Instrument Design and Performance for Optical/Infrared Ground-based Telescopes,
Masanori Iye, Alan F. M. Moorwood, Editors, Proceedings of SPIE Vol. 4841 (2003)

2. ADAPTIVE OPTICS AND HIGH RESOLUTION SPECTROSCOPY

2.1 Characteristics of the adaptively corrective image

Many of the recent AO systems incorporate both low order (tip-tilt) and high order (deformable mirror) correction. The AO system at the 2.5m telescope on Mt. Wilson uses natural guide stars (NGS) and a 241-actuator deformable mirror to provide high angular resolution imaging at visible wavelengths.[7] The ability of such systems to concentrate flux in the diffraction-limited core of diameter ~ λ/D is dependent not only on instantaneous seeing conditions as described by the atmospheric turbulence coherence length r_0, but also on wind velocity, the angle between the guide star and the object (atmospheric anisoplanatism), and the brightness of the guide star. The remaining energy is contained within the outer portion of the image, the seeing-limited halo. For the AO system at Mt. Wilson the energy in the core, as approximated by the Strehl ratio, is only about 9% for summer observing conditions, while the encircled energy within a 0.2" diameter is about 31%. In contrast, the AO system at the SOR 3.5m telescope is capable of concentrating up to ~40% of the energy in the core. Different slit widths or fiber diameters would be required when using the spectrograph with other AO systems, as discussed further in the section on fiber parameters.

2.2 Advantages of a spectrograph utilizing AO corrected images

Several important performance improvements can be realized when a spectrograph is used with adaptively corrected images.

- Since slit width or fiber diameter is normally matched to image diameter for highest throughput, and since spectral resolution is inversely proportional to slit width, the use of AO images permits the attainment of near diffraction-limited resolution without loss of light. While the use of a slit width less than that of a seeing-limited image would provide similar high spectral resolution, most of the light from the object would be lost.
- Although devices such as image slicers permit narrow slit widths without the corresponding loss of light noted above, the sliced images have to be mounted in the spatial direction on the detector, greatly limiting the wavelength coverage per exposure.
- The spectral resolution of a spectrograph coupled to a telescope is proportional to collimated beam diameter and inversely proportional to telescope objective diameter and image diameter (slit width). With seeing limited images, the image diameter is fixed regardless of objective size, so larger telescopes require larger collimators to maintain constant resolution. When using AO corrected images, however, the image diameter decreases with increasing objective size, so that high resolution spectrographs can be constructed with more conventional size collimators and gratings.
- Narrower AO corrected images permit the stacking of a greater number of echelle orders within the format of the detector, meaning that greater wavelength coverage per exposure is possible for a given size detector.
- The greater wavelength coverage per exposure eliminates the need for grating angle adjustments and the potential associated systematic errors.
- Spectrographs designed for AO corrected images can have higher efficiency than traditional instruments because of lower slit losses.
- For traditional seeing-limited spectrographs on large telescopes, maintaining wavelength coverage per exposure with the required large collimated beams requires faster camera optics, usually equating to a more expensive instrument. Spectrographs for AO corrected beams can utilize slower, less expensive camera optics.
- Astronomical phenomena with smaller spatial structure can be recorded.
- The narrower entrance slit required reduces sky background, especially in the IR.

3. ACES INSTRUMENT DESCRIPTION

3.1 Optical design

The ACES instrument has been described in earlier papers, and will only be summarized here. Fig. 1 shows the optical layout, utilizing an R2 echelle grating in near Littrow configuration with a 21° prism used in double pass for cross dispersion. Table 1. lists the optical parameters. The design is novel in that a Maksutov type corrector is used to correct

aberrations of the spherical collimator/camera objective, with a field corrector employed to remove field curvature and residual coma and astigmatism.[8]

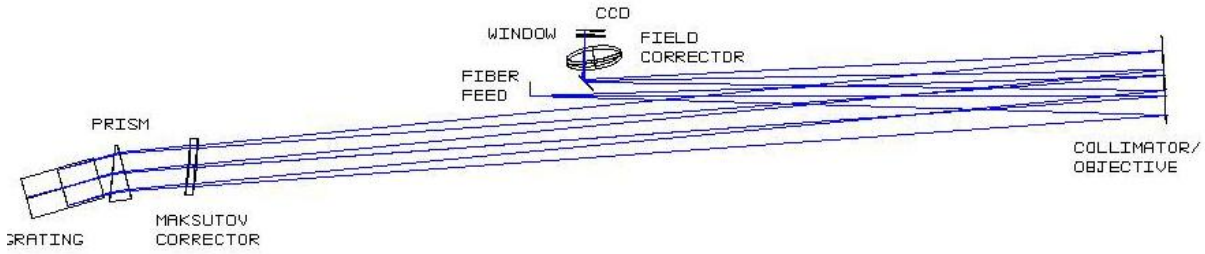

Fig. 1. Optical Layout

Table 1. Optical Parameters

Parameter	Value
Configuration	Near Littrow
Collimator	Spherical mirror (used with Maksutov corrector)
Collimated beam diameter	254mm
Primary disperser	R2 echelle, 116 x 242mm ruled area, 23.2 l/mm
Cross disperser	21° BK7 Prism
Camera focal length	1.9m
Spectrograph focal ratio	F/16
Wavelength range	~400-1000nm
Wavelength coverage per exposure	~470nm
Input slit width	10μm diameter optical fiber
Detector	Marconi CCD44-82, 2048x4096, 15μm pixels
Sampling	2.5 pixels for 40μm projected fiber diameter

3.2 Optomechanical Design

The instrument is mounted on a standard optical bench utilizing Nitrogen-filled flotation legs for vibration isolation. Fig. 2 shows an overhead view of the instrument set up on a 4’ x 8’ table at Mt. Wilson; a 4’ x 10’ table has been used for testing at Steward. The optics are assembled in modules for portability and ease of alignment. The center module, a 30” x 30” optical breadboard, mounts the fiber feed assembly, fold flat, field corrector, and detector. The module on the right end of the table holds the collimator/objective mirror in a tip-tilt mount. The module on the left houses the grating and prism in a common box as well as the Maksutov corrector. When observing, an enclosure is installed over the table to reduce stray light.

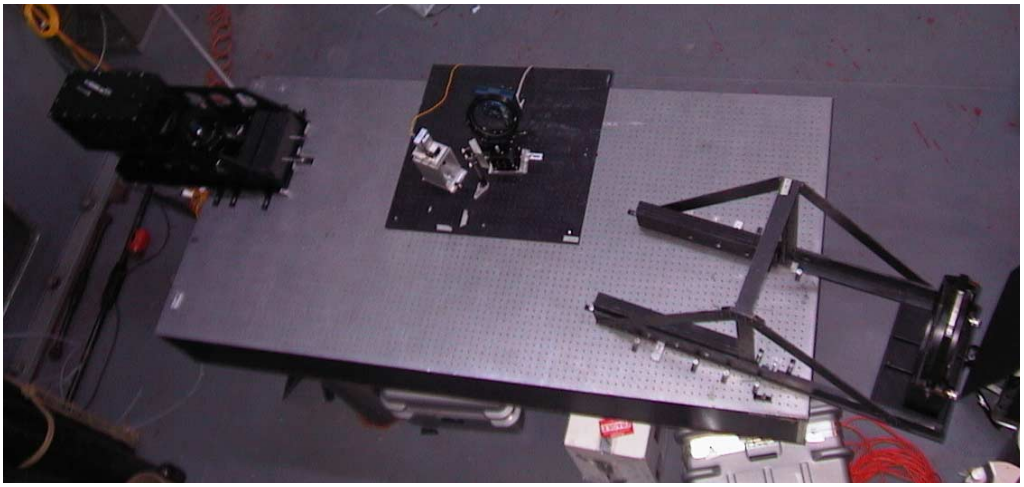

Fig. 2. Overhead view of the spectrograph layout on a 4’ x 8’ optical table.

3.3 Fiber feed

The fiber feed assembly (Fig. 3), mounted at the bent Cassegrain focus of the 2.5m telescope when observing at Mt. Wilson, provides for alignment of the AO corrected beam with the fiber, as well as focal ratio matching of the F/42 AO system to F/4 for optimal coupling to the fiber. The AO focal plane is made coincident with an aperture mirror that incorporates a 100μm hole, corresponding to 0.2 arcsec on the sky,. The field surrounding the target object is viewed with a reimaging lens and CCD camera, and the aperture is made coaxial with the focal ratio converter and fiber using x & y stages. A z-axis stage has been added to the previous design to permit accurately positioning the aperture plane at the correct conjugate distance from the focal ratio converter objective. The objective is mounted on x-y-z stages to permit aligning to the fiber axis and focusing, and the fiber coupler is mounted on a tip-tilt stage to permit aligning with the incoming beam. The objective and fiber coupler mounts are fitted with piezoelectric picomotors to permit remote adjustment with a hand-held controller device.

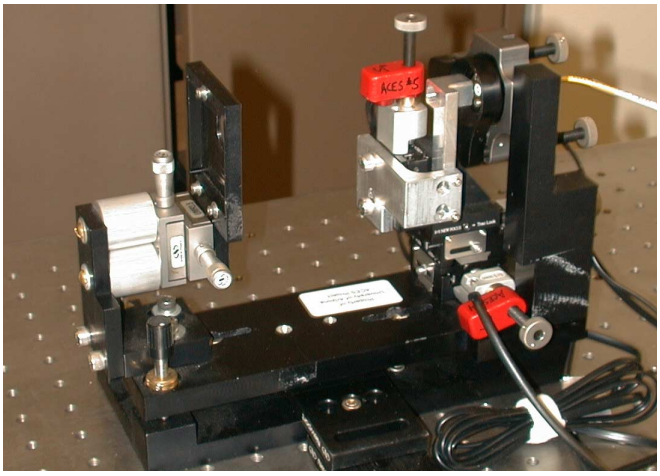

Fig. 3. Fiber feed assembly showing x-y mount for aperture mirror, x-y-z mount for objective, and tip-tilt mount for fiber connector. Optical fiber can be seen exiting to the right.

4. MARCONI CCD AND DEWAR

4.1 Dewar and CCD mechanical interface

An ND-5 liquid nitrogen dewar manufactured by Infrared Labs is used to cool the CCD. In previous engineering runs, the orientation of the CCD and dewar window necessitated mounting the dewar on its side to correctly orient the echellogram on the detector, and this limited the effective liquid nitrogen capacity of the dewar. The window and CCD orientation have now been rotated 90° to align the axis of the CCD with the echellogram in such a way that the dewar can be mounted in an upright position to allow complete filling. Damage to the original Loral 2048x4096 CCD resulting from an apparent ESD event necessitated replacement of the detector, and a Marconi CCD44-82 device, also 2048x4096 with 15μm pixels, was selected. The mounting of the Marconi device, which is designed for mosaics, is substantially different from that of the Loral chip, and is based on a series of studs with integral spacers, along with precision alignment pins. The dewar cold finger was modified and an Invar interface plate fabricated to match the Invar case of the CCD. Fig. 4 shows details of the mounting, including location of the temperature sensors and heater.

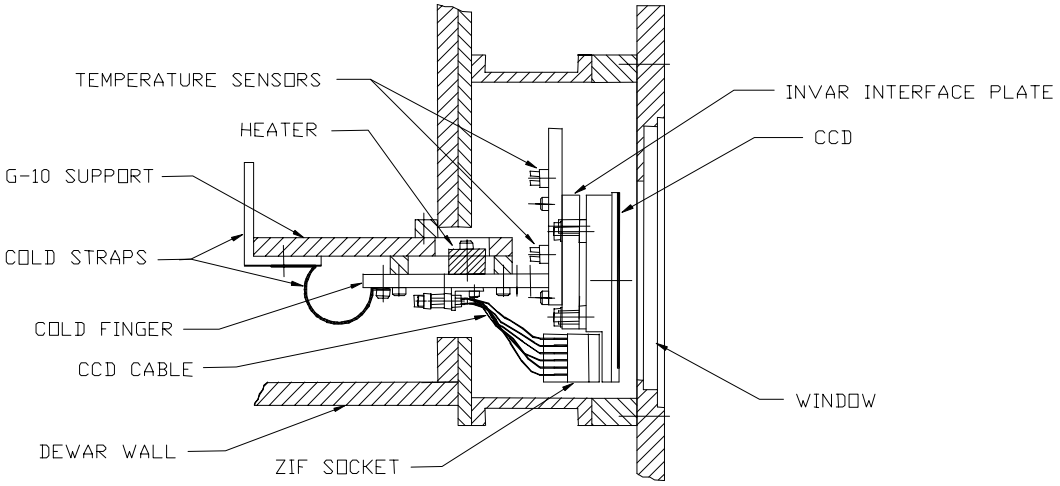

Fig. 4. Section through dewar showing Marconi CCD on cold finger

4.2 CCD electrical interface

The CCD package utilizes a 40-pin pin grid array (PGA), which is accessed through a custom zero insertion force (ZIF) socket. We connected to the ZIF socket by soldering wires directly to the socket leads, using a special wire guide block developed by the socket manufacturer to support the wires in such a configuration. Some users have interfaced to the socket with a printed wiring board (PWB), and we may change to that configuration if problems are encountered with the direct soldered wires.

4.3 CCD controller, operating parameters and measured performance

A San Diego State University Generation I controller is used to operate the CCD. This family of controllers is designed to provide adjustable clock and bias voltages for operation of one or more detectors, with communication via a VME interface board. The thinned, back-illuminated CCD44-82 is equipped with two output amplifiers and is divided into left and right sections for readout at speeds up to 1 MHz. We presently have only a single analog readout board in the controller and are reading out through one amplifier at 40 kHz, but plan to add a second analog channel to the controller

to permit readout through both channels. The optional FET output buffer is not used. Table 2 lists the current operating parameters.

Table 2. Marconi CCD44-82 operating parameters

Marconi parameter name	Data sheet range (V)	Marconi test value (V)	ACES operating value (V)
V_{SS}	0 – 10.0	6.0	-0.3
ODL, ODR	27.0 – no max.	28.0	23.0
RDL, RDR	15.0 – no max.	18.0	13.0
OG1L, OG1R	1.0 – 4.0	3.0	-5.0
OG2L, OG2R	OG2 = OG1 + 1 V	4.0	-4.0
DDL, DDR	22.0 – 26.0	20.0	Not used
Iϕ1, Iϕ2, Iϕ3 (parallel clocks)	8.0 – 14.0 (high)	10.0	2.0
Rϕ1, Rϕ2, Rϕ3 (serial clocks)	9.0 – 15.0 (high)	11.0	2.0
ϕRL, ϕRR (reset gate)	9.0 – 15.0 (high)	12.0	2.5
ϕSWL, ϕSWR	9.0 – 15.0 (high)	Not reported	2.0

The CCD was tested at the University Of Arizona Imaging Technology Laboratory. The photon transfer technique was used for gain and read noise calibration.[9] Illumination was with a 21" integrating sphere fed by a 150 W Hg-Xe lamp. Images were characterized at 400, 600, and 900nm using an approximately 100 A wide bandpass from a monochromator. Voltages and clocking patterns for the SDSU Gen 1 controller were optimized for lowest noise and minimal cosmetics effects. Tests were carried out at a temperature of approximately -100 C. Results of testing by the manufacturer and the University Of Arizona are tabulated in Table 3.

Table 3. Marconi CCD44-82 performance

Parameter	Requirement	Marconi test value	ACES operating value
Q.E. @ 173K at 350nm	>40 %	65.7 %	Not measured
400nm	>70 %	91.1 %	Not measured
500nm	>80 %	91.5 %	Not measured
650nm	>75 %	85.3 %	Not measured
900nm	>25 %	28.9 %	Not measured
Annealing pattern at 400nm	<10 %	Not measured	3%
Fringing at 900nm	<10 %	Not measured	6%
Output amplifier responsivity	>4.5 μV/e^-	6.46/6.30 μV/e^- left/right	Not measured
Gain	(system function)	N/A	1.1 e^-/DN
Readout noise	<4.0 rms e^-	2.2/2.2 rms e^- left/right	3.3 rms e^-
Non-linearity	<5.0 %	0.1/1.0 % left/right	Not measured
Pixel full well capacity	>150k e^-	Not measured	>70k e^- (ADC limited)
CTE (serial)	>99.999 %	99.9995/99.9996 % L/R	Not measured
CTE (parallel)	>99.999 %	99.9998 %	Not measured
Mean dark signal	<1.0 e^-/pixel/h at 153K	0.143 e^-/pixel/h	Not measured
White pixels*	<500 (Grade 1)	1	Not measured
Dark pixels*	Not specified	22	Not measured
Total pixel defects	<1250 (Grade 1)	23	Not measured
Traps (>200e^- at 173K)	<30 (Grade 1)	2	Not measured
Total column defects*	<6 (Grade 1)	1	1
Device flatness	Not specified	31 μm peak to valley	Not measured
*measured at 173K			

5. OPTICAL FIBER AND THE MODAL NOISE PROBLEM

5.1 Single mode optical fiber for coupling to astronomical instruments

Studies have previously been carried out at Steward Observatory to determine the properties of optical fibers typically used in communications, and their applicability to science instruments.[10] In particular, a commercial OH dry 8 μm core diameter fiber of fused silica used primarily for single mode communication at 1.5 μm was characterized in terms of focal ratio degradation, the decrease in focal ratio with length, which is an important factor in recovering maximum flux at the spectrograph input. Tests showed that the output focal ratio was almost independent of input focal ratio, consistent with single-mode fibers. For an F/4 input, about 80% of the input photons emerge within an F/4 cone. For imaging with the NGS AO system at the 2.5m telescope, an aperture of 100μm diameter is used at the fiber feed, corresponding to 0.2arcsec on the sky with the F/42 beam. For feeding the fiber at F/4, the required fiber diameter is then 10μm, with a 10X objective functioning as the focal ratio converter. At the fiber output, a 4X objective converts the cone to F/16 to match the focal ratio of the spectrograph. Use of a projected aperture size that is several times the diffraction-limited core diameter is a compromise in which spectral resolution is sacrificed in order to capture a greater percentage of the total flux. Inclusion of a greater percentage of flux in the core by systems with better high-order correction would permit substitution of a smaller projected aperture (corresponding to a smaller diameter fiber) and would result in a higher spectral resolution.

5.2 Evidence of modal noise

During any observation run with the spectrograph, flat field images are taken for detector characterization, and it is expected that all flats should be identical apart from readout noise and photon noise. Flat fields taken with ACES show a distinct irradiance modulation along most of the orders, as shown in Fig. 5, where a Tungsten halogen source was used. The modulation has a period of a few Angstroms along the dispersion axis. Fig. 6 is an IRAF plot of the signal level versus column number (wavelength) for a particular echelle order, showing the magnitude of the modulation. The modulation would not necessarily be a problem in itself if it were identical in all images, but it appears to be time-dependent. Flat fields taken with identical setups but at different times show a periodic pattern when divided together, whereas a flat line would be expected, apart from photon noise.[6] A recent paper authored by a group using multimode fiber in spectroscopy attributes the effect to 'modal noise' explainable because the fiber is acting as a waveguide and the transmission modes are visible as spot patterns on the output face of the fiber.[5] In the multimode application described, bending of a section of the fiber was found to randomize the pattern by "scrambling" the modes, thereby eliminating the problem.

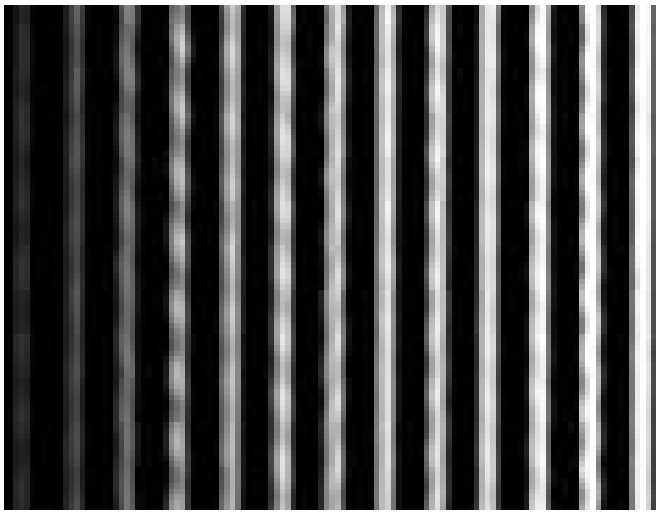

Fig. 5. Echelleogram orders showing irradiance modulation

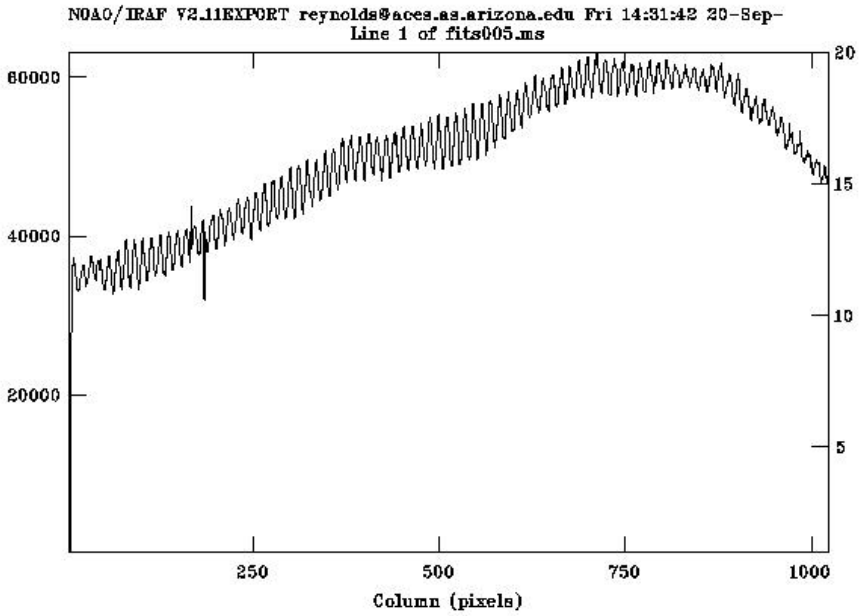

Fig. 6. IRAF irradiance plot showing wavelength-dependent variation with the fiber static.

5.3 Eliminating the modal noise problem

In the case of ACES, however, the fiber is carrying only a few tens of modes, depending on the wavelength, and any mode coupling techniques are believed to be less effective. Furthermore, bending of the fiber should always lead to coupling of energy from guided modes to radiation modes, resulting in loss of a portion of the transmitted flux.[11] We have recently experimented with varying the length of the fiber during the exposure rather than bending it, accomplished by manually stretching the fiber. Fig. 7 shows the reduction in modulation amplitude observed for the same echelle order depicted in Fig. 6 when the 24.4m fiber length was varied by ~ 5mm during the exposure.

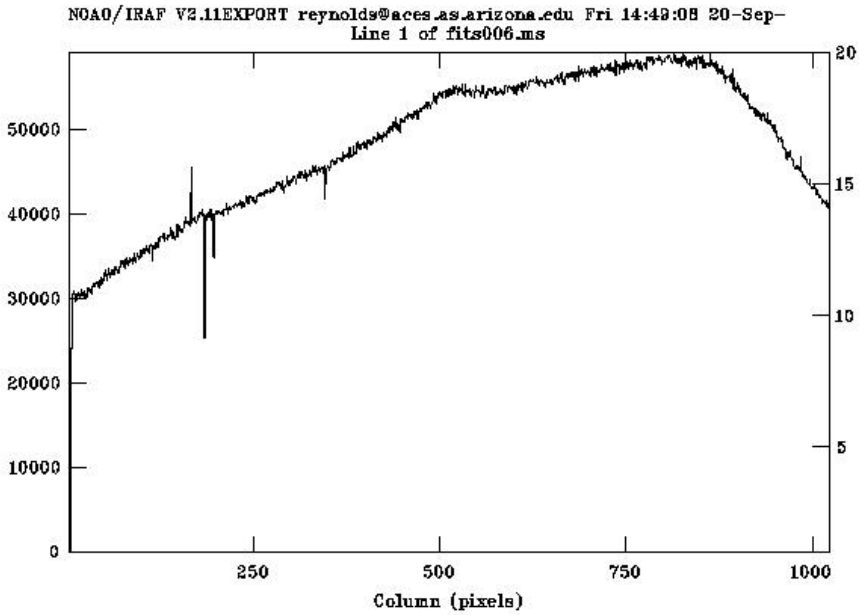

Fig. 7. Irradiance plot showing reduced variation when the fiber length is varied during the exposure.

To measure the amount of power that could be removed from the observed periodicity, IRAF was used to compute power spectral densities (PSD) for the orders. Fig. 8 shows the PSD plots for the cases with static fiber and length-varied fiber with power on a log scale, indicating a reduction in power of approximately 2 ½ orders of magnitude at the frequency of interest.

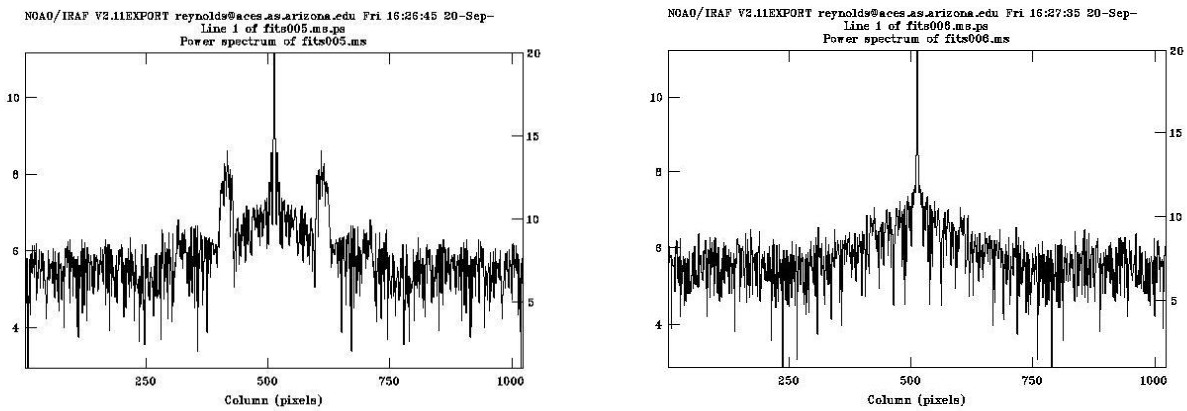

Fig. 8. Power spectral density plots of the irradiance variations of Fig's. 6 & 7 showing reduction in power at the subject frequency, located at column no's. 420 and 610 in these plots where the center of the x axis represents zero frequency.

We plan to investigate the dependence of this power reduction on the variation in length and on the length of fiber stretched, and are attempting to compute the mode structure at selected frequencies to see whether the variation in fiber length should be expected to produce the observed reduction in the modulation phenomenon. If further testing confirms the results, we will fabricate a device to automate the stretching of the fiber. The method is attractive in that it offers a potential technique for solving the problem without the radiation loss inherent in techniques relying on bending

6. SUMMARY

Testing of a slit-fed echelle spectrograph at the SOR 1.5m telescope has demonstrated that high resolution can be achieved by mating a spectrograph to a telescope equipped with high-order adaptive optics. A fiber-fed version of the same instrument at the Mt. Wilson 2.5m telescope showed that a near single-mode optical fiber could be used for coupling. The high resolution ($R \approx 190{,}000$) of a faster version of the spectrograph, designed for higher throughput, has been proven at the 2.5m telescope, and a new high-quantum efficiency CCD has been installed. Commissioning runs with the instrument showed a fiber transmission problem that prevents effective flat-fielding, and tests were undertaken to determine whether published techniques were applicable to the problem. Subsequent laboratory testing of a fiber stretching technique has shown promise for solving the problem. We plan further tests on this technique and fabrication of equipment to implement it. These modifications should permit the spectrograph to realize its full potential at telescopes equipped with the most advanced high-order AO systems.

ACKNOWLEDGEMENTS

The authors wish to thank the operating personnel at the 2.5m telescope of Mount Wilson Observatory, including Claudia Spaeth Beaudoin, P. J. Goldfinger, Kirk Palmer, Joe Russell, and Nils Turner (CHARA). Greg Winters and Michael

Bradley of Steward Observatory provided design and fabrication assistance for the CCD cable. Dave Baxter of Steward's Imaging Technology Laboratory assisted in dewar and CCD testing and participated in many useful discussions on dewar and cable design. This work was supported by NSF Grant # 9731176.

REFERENCES

1. J. Ge et al., "An optical ultrahigh resolution spectrograph for use with adaptive optics", *Adaptive Optics*, Vol. 13, OSA Technical Digest Series, pp. 122-133, Optical Society Of America, Washington DC, 1996.
2. J. Ge et al., "A prototype very high resolution spectrograph with adaptive optics", *BAAS*, **28**, pp. 905, 1996.
3. W. D. Heacox, "On the application of optical-fiber image scramblers to astronomical spectroscopy", *AJ*, **92**, pp. 219-229, 1986.
4. J. Ge et al., "Adaptive optics high resolution spectroscopy: present status and future directions", *Imaging the Universe In Three Dimensions: Astrophysics With Advanced Multi-Wavelength Imaging Devices*, ed. Van Breugel and Bland-Hawthorn, ASP Conference Series, Vol. 195, pp. 568-572, 2000.
5. Jacques Baudrand and Gordon A. H. Walker, "Modal noise in high-resolution, fiber-fed spectra: a study and simple cure", *PASP*, **113**, pp.851-857, 2001.
6. Matthew Kenworthy, "Report on fiber flexure tests at Mount Wilson June 2001", *Steward Observatory Internal Report*, pp. 1-8, 2001.
7. J. Christopher Shelton, T. Schneider, Daniel McKenna, Sallie L. Baliunas, "First tests of the Cassegrain adaptive optics system of the Mount Wilson 100-in telescope", *Adaptive Optics Systems and Applications*, ed. Tyson and Fugate, Proc. SPIE, **2534**, pp. 72-77, 1995.
8. Jian Ge et al., "Adaptive optics high resolution spectroscopy: present status and future direction", A*daptive Optics Systems and Technology*, ed. Tyson and Fugate, Proc. SPIE, **3762**, pp. 174-183, 1999.
9. James R. Janesick, *Scientific Charge-Coupled Devices*, pp. 101-107, SPIE Press, Bellingham. WA. 2001.
10. Jian Ge, Roger Angel, Chris Shelton, "Optical spectroscopy with a near dingle-mode fiber feed and adaptive optics", *Optical Astronomical Instrumentation*, ed. D'Odorico, Proc. SPIE, **3355**, pp. 253-263, 1998.
11. G. Keiser, *Optical Fiber Communications*, pp. 93-96, McGraw-Hill Inc., New York, 1991.

Further author information:
R.O.R. (correspondence): Email : reynolds@as.arizona.edu; phone: 520-621-1833; fax: 520-621-0943; Steward Observatory Room N430, 933 N. Cherry Ave., University Of Arizona, Tucson, AZ, 85721.
M.L.-H. mhart@as.arizona.edu
M.P.L. mlesser@as.arizona.edu
M.A.K. matt@physics.uc.edu
J.G. jian@astro.psu.edu